Program # 225.04
Poster # Q2

Using Quantitative Anisotropy and Computational Analysis Across 174 Brain Areas to Identify Changes in Gray Matter Microarchitecture in the APOE Knock-Out Rat: Evidence of Gender Differences and Alterations in Cortico/Thalamic and Cerebellar Connectivity

Ju Qiao[1], Codi Gharagouzloo[1], Praveen Kulkarni[2], Liam Timms[1], Kevin Gamber[3], Mark Nedelman[4], Srinivas Sridhar[1], Craig F Ferris[2]

[1] Nanomedicine Science and Technology Center, Northeastern University [2] Center for Translational NeuroImaging, Northeastern University, Boston, MA
[3] Horizon Discovery, St Louis MO [4] Ekam Imaging, Boston, MA, USA

horizon

Northeastern University
Center for Translational Neuro-imaging

Ekam Imaging
Advancing Early Drug Discovery

Abstract

In the central nervous system, apolipoprotein E (APOE) is produced in glia and functions in the transport of cholesterol to neurons via APOE receptors. The absence or dysregulation of this lipoprotein increases risk for vascular disorders and Alzheimer's disease (AD). The recent development of transgenic homozygous APOE -/- knock out (KO) rats provided an opportunity to apply a new imaging methodology "in vivo neuropathology" to non-invasively study subtle changes in gray matter microarchitecture in WT and KO female and male rats using quantitative anisotropy across 174 brain regions. In addition, T1 and T2 relaxivity measures were collected across these brain regions and comparisons made between gender and the APOE genotype. All studies were done on a Bruker 7T MR scanner while rats were anesthetized with 2% isoflurane.

Both males and female APOE KO rats showed over 40 brain areas with altered T1 relaxivity as compared to gender matched WT controls. The entire cerebellum and deep cerebellar nuclei were affected as were many of their afferent and efferent connections in brainstem and pons. There was little difference in T1 measures between genders. Changes in T2 relaxivity between APOE genotypes were less pronounced and numbered only 10 in females and18 in males. Again areas of the cerebellum and their afferent and efferent connections were involved. Quantitative anisotropy showed clear male/female differences. In the males this imaging technique complemented the relaxivity measures as the cerebellum again showed differences between APOE genotypes for fractional anisotropy and radial diffusivity. In addition, many thalamic areas and their cortical connections were altered. In females the changes were fewer and localized primarily to hypothalamus and amygdala.

In this study multiple non-invasive MRI protocols were used to identify putative changes in gray matter microarchitecture across 174 brain areas in a rat model of AD. The changes were both gender and APOE specific. Rats, male and female, lacking apolipoprotein E showed significant differences in cerebellum and its afferent and efferent connections for measures of T1. This profile was consistent for males for T2 and indices of anisotropy but different for females. There was little evidence of any changes in the hippocampal complex between gender and APOE genotype. Brains were harvested and are undergoing immunhistochemical analysis for glial fibrillary associated protein and activated microglia to assess neuroinflammation in areas identified with these imaging protocols.

Materials & Methods

Experimental Design

Wild-type (WT) (n = 12) and APOE Ɛ4 (n = 12) , male and Female, rats were obtained from Horizon Discovery. Studies were performed on a Bruker BioSpec 7T / 20cm USR. Four types of scans were acquired 1) High resolution Anatomy scans for volumetric assesment 2) T2 map 3) Diffusion Tensor imging 4) Functional Connectivity scans. All animals were studied at 4-5 months of age.

Diffusion Tensor Imaging

DTI was acquired with a diffusion-weighted (DW) spin-echo echo-planar-imaging (EPI) pulse sequence having the following parameters: TR/TE 00/20 ms, eight EPI segments, and 10 non-collinear gradient directions with a single b-value shell at 1000 s/mm^2 and one image with a b-value of 0 s/mm^2 (referred to as b0). Geometrical parameters were: 60 slices, each 0.313 mm thick (brain volume) and with in-plane resolution of 0.313×0.313 mm^2 (matrix size 96×96; FOV 30 mm^2). The imaging protocol was repeated two times for signal averaging. Each DTI acquisition took 44 min and the entire MRI protocol lasted about 1 hour 28 min.

T2 relaxometry

Multi echo images were acquired using MSME pulse sequence (TR= 5.4 sec and TE: 11, 22, 33, 44, 55, 66, 77, 88, 99, 110 msec.) Images were acquired with a field of view [FOV] 3 cm2, data matrix = 128×128×20 slices, thickness = 1 mm. T2 measurements were computed using Paravision 5.1 software (Bruker, Billerica, Massachusetts) by fitting absolute signal at particular TE.

Image Analysis

Image analysis included DTI analysis of the DW-3D-EPI images to produce the FA, ADC and RA maps. DTI analysis was implemented with Matlab (©Mathworks, USA) and **MedINRIA (1.9.0; http://www-sop.inria.fr/asclepios/software/MedINRIA/index.php)** software. Because sporadic excessive breathing during DTI acquisition can lead to significant image motion artifacts that are apparent only in the slices sampled when motion occurred, each image (for each slice and each gradient direction) was automatically screened, prior to DTI analysis, for motion artifacts. Following the elimination of acquisition points with motion artifacts, the remaining acquisition points were corrected for linear (motion) and non-linear (eddy currents/susceptibility) artifacts using SPM8 (Welcome Trust Centre for Neuroimaging, London, UK).

Materials & Methods

Each subject was registered to a 3D segmented and annotated rat brain atlas (Ekam Solutions LLC, Boston MA.). The alignment process was facilitated by an interactive graphic user interface EVA. The affine registration involved translation, rotation, and scaling in all 3 dimensions independently. The matrices that transformed the subject's anatomy to the atlas space were used to embed each slice within the atlas. All transformed pixel locations of the anatomy images were tagged with the segmented atlas regions, creating a fully segmented representation of each subject. T1 parameter values for each ROI was computed based on each segmented map.

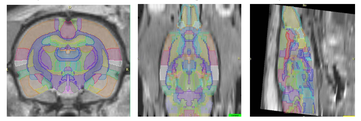

Diffusion Tensor Imaging

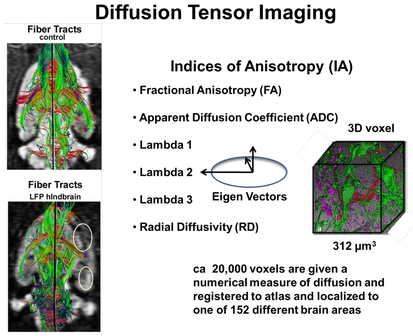

T2 Relaxometry Probability Maps Comparing Sex Differences Between APOE KO and APOE4 Genotypes

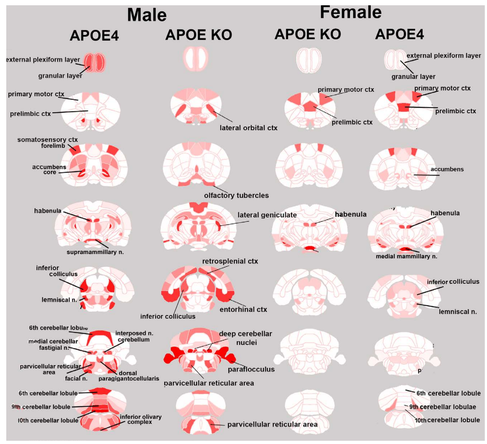

Main Results

Probability Maps Comparing Sex Differences in APOE KO Rats with MRI : Measures of T2 Relaxometry, Fractional Anisotropy, Radial Diffusivity and Axial Diffusivity

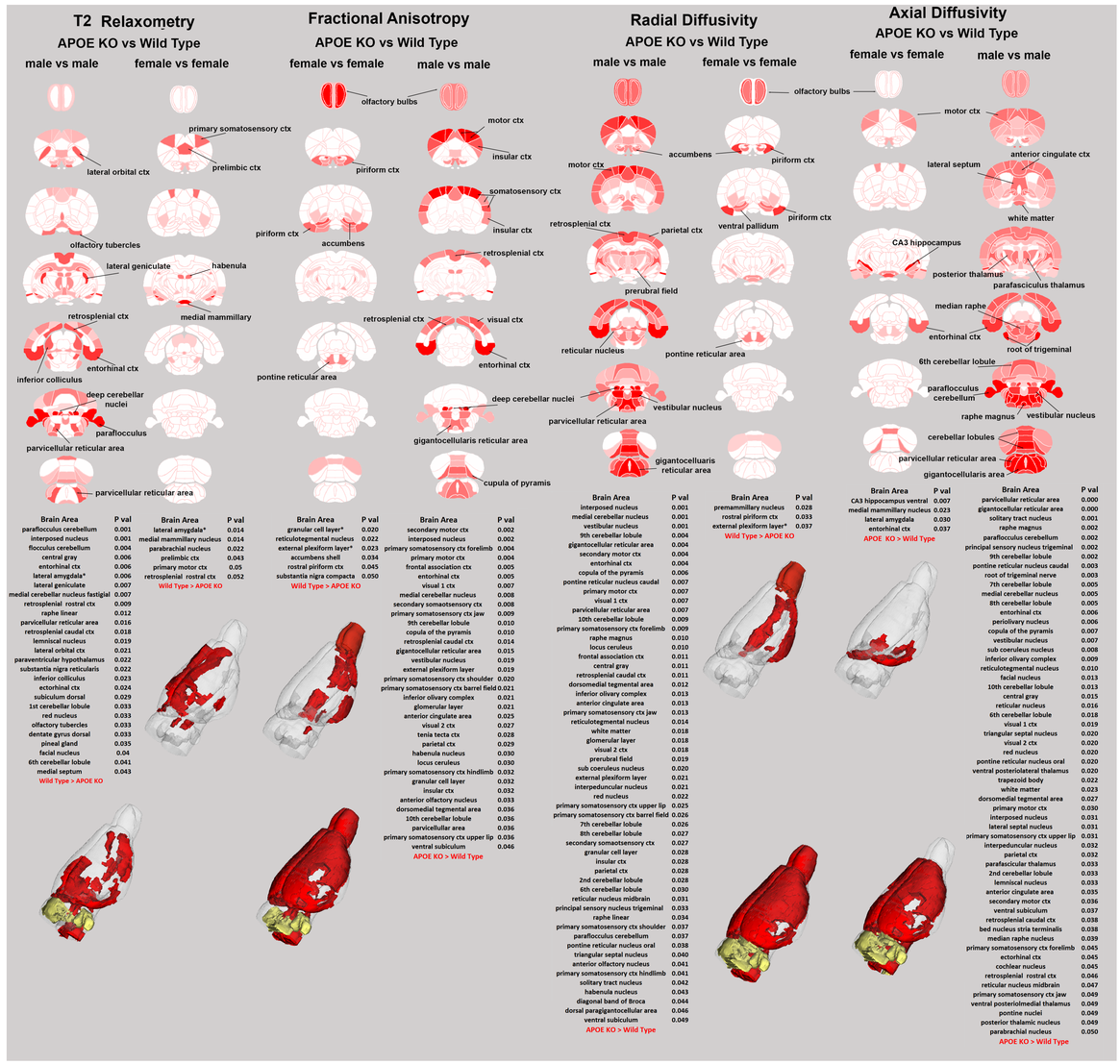

Brain Area	P val	Brain Area	P val
parafloccullus cerebellum	0.001	lateral amygdala*	0.014
interposed nucleus	0.001	medial mammillary nucleus	0.014
flocculus cerebellum	0.004	parabrachial nucleus	0.022
central gray	0.006	prelimbic ctx	0.043
entorhinal ctx	0.006	primary motor ctx	0.05
lateral amygdala*	0.006	retrosplenial rostral ctx	0.052
lateral geniculate	0.007		
medial cerebellar nucleus fastigial	0.007		
retrosplenial rostral ctx	0.009		
raphe linear	0.012		
parvicellular reticular area	0.016		
retrosplenial caudal ctx	0.018		
lemniscal nucleus	0.019		
lateral orbital ctx	0.021		
paraventricular hypothalamus	0.022		
substantia nigra reticularis	0.022		
inferior colliculus	0.023		
ectorhinal ctx	0.024		
subiculum dorsal	0.029		
1st cerebellar lobule	0.033		
red nucleus	0.033		
olfactory tubercles	0.033		
dentate gyrus dorsal	0.033		
pineal gland	0.035		
facial nucleus	0.04		
6th cerebellar lobule	0.041		
medial septum	0.043		

Wild Type > APOE KO

Brain Area	P val	Brain Area	P val
granular cell layer*	0.020	secondary motor ctx	0.002
reticulotegmental nucleus	0.022	interposed nucleus	0.002
external plexiform layer*	0.023	primary somatosensory ctx forelimb	0.004
accumbens shell	0.034	primary motor ctx	0.004
rostral piriform ctx	0.045	frontal association ctx	0.005
substantia nigra compacta	0.050	entorhinal ctx	0.005
		visual 1 ctx	0.007
		medial cerebellar nucleus	0.008
		secondary somatosensory ctx	0.008
		primary somatosensory ctx jaw	0.009
		9th cerebellar lobule	0.010
		copula of the pyramis	0.010
		retrosplenial caudal ctx	0.014
		gigantocellular reticular area	0.015
		vestibular nucleus	0.019
		external plexiform layer	0.019
		primary somatosensory ctx shoulder	0.020
		primary somatosensory ctx barrel field	0.021
		inferior olivary complex	0.021
		glomerular layer	0.021
		anterior cingulate area	0.025
		visual 2 ctx	0.027
		tenia tecta ctx	0.028
		parietal ctx	0.029
		habenula nucleus	0.030
		locus ceruleus	0.030
		primary somatosensory ctx hindlimb	0.032
		granular cell layer	0.032
		insular ctx	0.032
		anterior olfactory nucleus	0.033
		dorsomedial tegmental area	0.036
		10th cerebellar lobule	0.036
		parvicellular area	0.036
		primary somatosensory ctx upper lip	0.036
		ventral subiculum	0.046

APOE KO > Wild Type

Brain Area	P val	Brain Area	P val
interposed nucleus	0.001	premammillary nucleus	0.028
medial cerebellar nucleus	0.001	rostral piriform ctx	0.033
vestibular nucleus	0.001	external plexiform layer*	0.037
9th cerebellar lobule	0.004		
gigantocellular reticular area	0.004		
secondary motor ctx	0.004		
entorhinal ctx	0.004		
copula of the pyramis	0.006		
pontine reticular nucleus caudal	0.007		
primary motor ctx	0.007		
visual 1 ctx	0.007		
parvicellular reticular area	0.007		
10th cerebellar lobule	0.009		
primary somatosensory ctx forelimb	0.009		
raphe magnus	0.010		
locus ceruleus	0.010		
frontal association ctx	0.011		
central gray	0.011		
retrosplenial caudal ctx	0.011		
dorsomedial tegmental area	0.012		
inferior olivary complex	0.013		
anterior cingulate area	0.013		
primary somatosensory ctx jaw	0.013		
reticulotegmental nucleus	0.014		
white matter	0.018		
glomerular layer	0.018		
visual 2 ctx	0.018		
prerubral field	0.019		
sub coeruleus nucleus	0.020		
external plexiform layer	0.021		
interpeduncular nucleus	0.021		
red nucleus	0.022		
primary somatosensory ctx upper lip	0.025		
primary somatosensory ctx barrel field	0.026		
7th cerebellar lobule	0.026		
8th cerebellar lobule	0.027		
secondary somatosensory ctx	0.027		
granular cell layer	0.028		
insular ctx	0.028		
parietal ctx	0.028		
2nd cerebellar lobule	0.028		
6th cerebellar lobule	0.030		
reticular nucleus midbrain	0.031		
principal sensory nucleus trigeminal	0.033		
raphe linear	0.034		
primary somatosensory ctx shoulder	0.037		
parafloccular cerebellum	0.037		
pontine reticular nucleus oral	0.038		
triangular septal nucleus	0.040		
anterior olfactory nucleus	0.041		
primary somatosensory ctx hindlimb	0.041		
solitary tract nucleus	0.042		
habenula nucleus	0.043		
diagonal band of Broca	0.044		
dorsal paragigantocellular area	0.046		
ventral subiculum	0.049		

APOE KO > Wild Type

Brain Area	P val	Brain Area	P val
CA3 hippocampus ventral	0.007	parvicellular reticular area	0.000
medial mammillary nucleus	0.023	gigantocellular reticular area	0.000
lateral amygdala	0.030	solitary tract nucleus	0.001
entorhinal ctx	0.037	raphe magnus	0.002
		parafloccullus cerebellum	0.002
		principal sensory nucleus trigeminal	0.002
		9th cerebellar lobule	0.002
		pontine reticular nucleus caudal	0.003
		root of trigeminal nerve	0.003
		7th cerebellar lobule	0.005
		medial cerebellar nucleus	0.005
		8th cerebellar lobule	0.005
		entorhinal ctx	0.006
		perioliviary nucleus	0.006
		copula of the pyramis	0.007
		vestibular nucleus	0.007
		sub coeruleus nucleus	0.008
		inferior olivary complex	0.009
		reticulotegmental nucleus	0.010
		facial nucleus	0.013
		10th cerebellar lobule	0.013
		central gray	0.015
		reticular nucleus	0.016
		6th cerebellar lobule	0.018
		visual 1 ctx	0.019
		triangular septal nucleus	0.020
		visual 2 ctx	0.020
		red nucleus	0.020
		pontine reticular nucleus oral	0.020
		ventral posteriolateral thalamus	0.020
		trapezoid body	0.022
		white matter	0.023
		dorsomedial tegmental area	0.027
		primary motor ctx	0.030
		interposed nucleus	0.031
		lateral septal nucleus	0.031
		primary somatosensory ctx upper lip	0.031
		interpeduncular nucleus	0.032
		parietal ctx	0.032
		parafascicular thalamus	0.033
		2nd cerebellar lobule	0.033
		lemniscal nucleus	0.033
		anterior cingulate area	0.035
		secondary motor ctx	0.036
		ventral subiculum	0.037
		retrosplenial caudal ctx	0.038
		bed nucleus stria terminalis	0.038
		median raphe nucleus	0.039
		primary somatosensory ctx forelimb	0.045
		ectorhinal ctx	0.045
		cochlear nucleus	0.045
		retrosplenial rostral ctx	0.046
		reticular nucleus midbrain	0.047
		primary somatosensory ctx jaw	0.049
		ventral posteriolmedial thalamus	0.049
		pontine nuclei	0.049
		posterior thalamic nucleus	0.049
		parabrachial nucleus	0.050

APOE KO > Wild Type

Summary

Male APOE KO

- Male APOE KO rats show a significant number of differences in MRI measures of microarchitecture as compared to wild type controls
- These differences were primarily in cerebral cortex, cerebellum and brainstem reticular activating system.
- No behavioral data or post mortem measures were taken.
- There were significant differences between APOE4 and APOE KO rats at five months of age

Female APOE KO

- Female APOE4 rats show very few significant differences in MRI measures of microarchitecture as compared to wild type controls
- These few differences were primarily in the olfactory system, and limbic cortex.
- No behavioral data or post mortem measures were taken.
- APOE4 and APOE KO females rats show no significant differences at 5 months of age.

This works was funded by SAGE Labs a Horizon Discovery Group Company and Ekam Imaging Inc.